Advances in Materials Research, *Vol. 5, No. 4 (2016) 223-244*
DOI: https://doi.org/10.12989/amr.2016.5.4.223

Effects of thickness stretching in FGM plates using a quasi-3D higher order shear deformation theory

Belkacem Adim[1,2] and Tahar Hassaine Daouadji[*1,2]

[1]*Département de génie civil , Université Ibn Khaldoun Tiaret; BP 78 Zaaroura, 14000 Tiaret, Algérie*
[2]*Laboratoire de Géomatique et Développement Durable, Université Ibn Khaldoun de Tiaret, Algérie*

(Received September 8, 2016, Revised December 20, 2016, Accepted December 21, 2016)

Abstract. In this paper, a higher order shear and normal deformation theory is presented for functionally graded material (FGM) plates. By dividing the transverse displacement into bending, shear and thickness stretching parts, the number of unknowns and governing equations for the present theory is reduced, significantly facilitating engineering analysis. Indeed, the number of unknown functions involved in the present theory is only five, as opposed to six or even greater numbers in the case of other shear and normal deformation theories. The present theory accounts for both shear deformation and thickness stretching effects by a hyperbolic variation of ail displacements across the thickness and satisfies the stress-free boundary conditions on the upper and lower surfaces of the plate without requiring any shear correction factor. Equations of motion are derived from Hamilton's principle. Analytical solutions for the bending and free vibration analysis are obtained for simply supported plates. The obtained results are compared with three-dimensional and quasi- three-dimensional solutions and those predicted by other plate theories. It can be concluded that the present theory is not only accurate but also simple in predicting the bending and free vibration responses of functionally graded plates.

Keywords: Functionally Graded Material; power law index; Higher-order Shear Deformation Theory; Navier solution

1. Introduction

The concept of functionally graded materials FGM was first introduced in 1984 by material scientists in the Sendai area of Japan. FGM is a class of composite materials that has continuous variation of material properties from one surface to another and thus eliminates the stress concentration found in laminated composites. Typically, the FGM is made from a mixture of a ceramic and a metal. FGMs are widely used in many structural applications such as mechanical, aerospace, civil, and automotive. When the application of FGMs increases, more accurate theories are required to predict their responses.

In the past three decades, researches on functionally graded material plates have received

∗Corresponding author, Professor, E-mail: daouadjitah@yahoo.fr
[a]Ph.D., E-mail: daouadjitah@yahoo.fr

http://www.techno-press.org/?journal=amr&subpage=7 ISSN: 2234-0912 (Print), 2234-179X (Online)

substantial attention, and an extensive spectrum of plate theories has been introduced based on the classical plate theory and shear deformation plate theory. The classical plate theory (CPT) neglects shear deformations and can lead to inaccurate results for moderately thick plates. This theory has been implemented for buckling analysis of FGM plates by Feldman and Aboudi (1997), Abrate (2008). First-order shear deformation theory (Reissner 1945, Mindlin 1951) considers the transverse shear deformation effects, but needs a shear correction factor in order to satisfy the zero transverse shear stress boundary conditions at the top and bottom of the plate. Many studies of the mechanical behavior of plates have been carried out using FSDT (Moradi 2012, Menaa 2012, Yaghoubi 2013 Gafour 2015, Baghdadi 2015, Rashidi 2012). To avoid the use of shear correction factors, several higher-order shear deformation plate theories have been proposed such as the theory propounded by Nelson and Lorch (1974) with nine unknowns, Lo *et al*. (1977) with eleven unknowns, Bhi-maraddi and Stevens (1984) with five unknowns, Reddy (1984) with five unknowns. Some higher order theories based on Carrera's unified Formulation (CUF) such as proposed in Refs (Neves 2012, Reddy 2000, Ait atman 2010, Abdelhak 2016, Ait yahi 2015, Boumia 2014, Bouazza 2015, Bensatallah 2016, Bellifa 2015) have been used also to study FGM structures. The majority of HSDTs used to investigate FGM plate mechanics have the same five unknowns. The resulting equations of motion are much more complicated than those yielded with FSDT. In addition, it should be noted that the above-mentioned two-dimensional plate theories discard the thickness stretching effect as they consider a constant transverse displacement through the thickness. This assumption is appropriate for thin or moderately thick FGM plates, but is inadequate for thick FGM plates (Qian 2004). The importance of the thickness stretching effect in FGM plates has been identified succinctly in the work of Carrera *et al*. (2011). This effect plays a significant role in thick FGM plates and should be taken into consideration.

In general, higher order shear and normal deformation theories which consider thickness stretching effect can be implemented using the unified formulation initially proposed by Carrera (2005). More detailed information and applications of the unified formulation can be found in the recent books by Carrera *et al*. (2011). Many higher order shear and normal deformation theories have been proposed in the literature (Matsunaga 2009). These theories are cumbersome and computation-ally expensive since they invariably generate a host of unknowns (e.g., theories by Reddy (2011) with eleven unknowns; and Neves *et al*. (2012) with nine unknowns). Although some well-known quasi-three-dimensional theories developed by Zenkour (2007) and recently by Mantari and Guedes Soares (2012) have six unknowns, they are still more complicated than the FSDT. Thus, there is a scope to develop an accurate higher order shear and normal deformation theory, which is relatively simple to use and simultaneously retains important physical characteristics. Indeed, Huu and Seung (2013) presented recently a quasi-3D sinusoidal shear deformation theory with only five unknowns for bending behavior of FGM plates.

In this paper, an efficient and simple quasi-3D trigonometric shear and normal deformation theory with only five unknowns is developed for FGM plates. Contrary to the four-variable refined theories elaborated in (Hassaine Daouadji 2015, Tlidji 2014, Bennoun 2016, Hamidi 2015, Mahi 2016, Adim 2016, Benferhat 2016), where the stretching effect is neglected, in the current investigation this so-called "stretching effect" is taken into consideration. Numerical examples are presented to verify the accuracy of the present theory.

2. Problem formulation

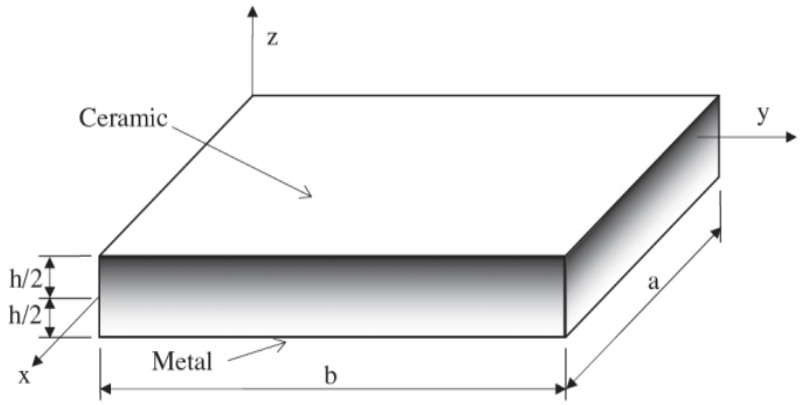

Fig. 1 Geometry of rectangular plate composed of FGM

2.1 The displacement field of the present theory is chosen based on the following assumptions (Fig. 1)

- The transverse displacements are partitioned into bending, shear and stretching components;
- The in-plane displacement is partitioned into extension, bending and shear components;
- The bending parts of the in-plane displacements are similar to those given by CPT;
- The shear parts of the in-plane displacements give rise to the trigonometric variations of shear strains and hence to shear stresses through the thickness of the plate in such a way that the shear stresses vanish on the top and bottom surfaces of the plate.

Based on these assumptions, the following displacement field relations can be obtained

$$\begin{aligned} u(x,y,z,t) &= u_0(x,y,t) - z\frac{\partial w_b}{\partial x} - f(z)\frac{\partial w_s}{\partial x} \\ v(x,y,z,t) &= v_0(x,y,t) - z\frac{\partial w_b}{\partial y} - f(z)\frac{\partial w_s}{\partial y} \\ w(x,y,z,t) &= w_b(x,y,t) + w_s(x,y,t) + g(z)w_z(x,y,t) \end{aligned} \tag{1}$$

Where u_0 and v_0 denote the displacements along the x and y coordinate directions of a point on the mid-plane of the plate; w_b and w_s are the bending and shear components of the transverse displacement, respectively; and the additional displacement w_z accounts for the effect of normal stress. In this study, the shape functions $f\{z\}$ and $g\{z\}$ are chosen based on the trigonometric function $\xi(z)$ proposed as (Hassaine Daouadji 2013)

$$f(z) = z - \xi(z), \quad \text{with}: \quad \xi(z) = \frac{3\pi}{2}h.\tanh\left(\frac{z}{h}\right) - \frac{3\pi}{2}z.\sec h^2\left(\frac{1}{2}\right) \tag{2}$$

$$g(z) = 1 - \frac{df(z)}{dz} \tag{3}$$

The non-zero strains associated with the new displacement field in Eq. (1) are

$$\begin{Bmatrix} \varepsilon_x \\ \varepsilon_y \\ \gamma_{xy} \end{Bmatrix} = \begin{Bmatrix} \dfrac{\partial u_0}{\partial x} \\ \dfrac{\partial v_0}{\partial y} \\ \dfrac{\partial u_0}{\partial y} + \dfrac{\partial v_0}{\partial x} \end{Bmatrix} - z \begin{Bmatrix} \dfrac{\partial^2 w_b}{\partial x^2} \\ \dfrac{\partial^2 w_b}{\partial y^2} \\ 2\dfrac{\partial^2 w_b}{\partial x \partial y} \end{Bmatrix} - f(z) \begin{Bmatrix} \dfrac{\partial^2 w_s}{\partial x^2} \\ \dfrac{\partial^2 w_s}{\partial y^2} \\ 2\dfrac{\partial^2 w_s}{\partial x \partial y} \end{Bmatrix} \tag{4a}$$

$$\begin{Bmatrix} \gamma_{yz} \\ \gamma_{xz} \end{Bmatrix} = (1 - \frac{\partial f(z)}{\partial z}) \begin{Bmatrix} \dfrac{\partial w_s}{\partial y} + \dfrac{\partial w_z}{\partial y} \\ \dfrac{\partial w_s}{\partial x} + \dfrac{\partial w_z}{\partial x} \end{Bmatrix} \tag{4b}$$

$$\varepsilon_z = \frac{\partial g(z)}{\partial z} \varepsilon_z^0 = g'(z).w_z \tag{4c}$$

2.2 Governing equations

Hamilton's principle is used herein to derive equations of motion. The principle can be stated in an analytical form as follows

$$\int_0^T (\delta U + \delta V - \delta K) dt = 0 \tag{5}$$

where δU is the variation of strain energy; δV is the variation of potential energy; and δK is the variation of kinetic energy. The variation of strain energy of the plate is calculated by

$$\delta U = \int_{-\frac{h}{2}}^{\frac{h}{2}} \int_A (\sigma_x \delta \varepsilon_x + \sigma_y \delta \varepsilon_y + \sigma_z \delta \varepsilon_z + \sigma_{xy} \delta \gamma_{xy} + \sigma_{yz} \delta \gamma_{yz} + \sigma_{xz} \delta \gamma_{xz}).dA.dz \tag{6}$$

$$\begin{aligned} \delta U = \frac{1}{2} \int_A [& N_x \frac{\partial u_0}{\partial x} - M_x^b \frac{\partial^2 w_b}{\partial x^2} - M_x^s \frac{\partial^2 w_s}{\partial x^2} + N_y \frac{\partial v_0}{\partial y} - M_y^b \frac{\partial^2 w_b}{\partial y^2} - M_y^s \frac{\partial^2 w_s}{\partial y^2} + N_z w_z \\ & + N_{xy} \left(\frac{\partial u_0}{\partial y} + \frac{\partial v_0}{\partial x} \right) - 2M_{xy}^b \frac{\partial^2 w_b}{\partial x \partial y} - 2M_{xy}^s \frac{\partial^2 w_s}{\partial x \partial y} + Q_x \left(\frac{\partial w_s}{\partial x} + \frac{\partial w_z}{\partial x} \right) + Q_y \left(\frac{\partial w_s}{\partial y} + \frac{\partial w_z}{\partial y} \right)] dA \end{aligned} \tag{7}$$

where A is the top surface and the stress resultants N; M, and Q are defined by

$$\begin{Bmatrix} N_x, & N_y, & N_{xy} \\ M_x^b, & M_y^b, & M_{xy}^b \\ M_x^s, & M_y^s, & M_{xy}^s \end{Bmatrix} = \int_{-h/2}^{h/2} (\sigma_x, \sigma_y, \sigma_{xy}) \begin{Bmatrix} 1 \\ z \\ f(z) \end{Bmatrix} dz \tag{8a}$$

$$N_z = \int_{-h/2}^{h/2} (\sigma_z) g'(z) dz \tag{8b}$$

$$(Q_x, Q_y) = \int_{-h/2}^{h/2} (\tau_{xz}, \tau_{yz}) g(z) dz \tag{8c}$$

where

$$N_x = A_{11}\frac{\partial u_0}{\partial x} + A_{12}\frac{\partial v_0}{\partial y} - B_{11}\frac{\partial^2 w_b}{\partial x^2} - B_{12}\frac{\partial^2 w_b}{\partial y^2} - B^s_{11}\frac{\partial^2 w_s}{\partial x^2} - B^s_{12}\frac{\partial^2 w_s}{\partial y^2} + X_{13}w_z \quad (9a)$$

$$N_y = A_{12}\frac{\partial u_0}{\partial x} + A_{22}\frac{\partial v_0}{\partial y} - B_{12}\frac{\partial^2 w_b}{\partial x^2} - B_{22}\frac{\partial^2 w_b}{\partial y^2} - B^s_{12}\frac{\partial^2 w_s}{\partial x^2} - B^s_{22}\frac{\partial^2 w_s}{\partial y^2} + X_{23}w_z \quad (9b)$$

$$N_{xy} = A_{66}\left(\frac{\partial u_0}{\partial y} + \frac{\partial v_0}{\partial x}\right) - 2B_{66}\frac{\partial^2 w_b}{\partial x\partial y} - 2B^s_{66}\frac{\partial^2 w_s}{\partial x\partial y} \quad (9c)$$

$$M^b_x = B_{11}\frac{\partial u_0}{\partial x} + B_{12}\frac{\partial v_0}{\partial y} - D_{11}\frac{\partial^2 w_b}{\partial x^2} - D_{12}\frac{\partial^2 w_b}{\partial y^2} - D^s_{11}\frac{\partial^2 w_s}{\partial x^2} - D^s_{12}\frac{\partial^2 w_s}{\partial y^2} + Y_{13}w_z \quad (9d)$$

$$M^b_y = B_{12}\frac{\partial u_0}{\partial x} + B_{22}\frac{\partial v_0}{\partial y} - D_{12}\frac{\partial^2 w_b}{\partial x^2} - D_{22}\frac{\partial^2 w_b}{\partial y^2} - D^s_{12}\frac{\partial^2 w_s}{\partial x^2} - D^s_{22}\frac{\partial^2 w_s}{\partial y^2} + Y_{23}w_z \quad (9e)$$

$$M^b_{xy} = B_{66}\left(\frac{\partial u_0}{\partial y} + \frac{\partial v_0}{\partial x}\right) - 2D_{66}\frac{\partial^2 w_b}{\partial x\partial y} - 2D^s_{66}\frac{\partial^2 w_s}{\partial x\partial y} \quad (9f)$$

$$M^s_x = B^s_{11}\frac{\partial u_0}{\partial x} + B^s_{12}\frac{\partial v_0}{\partial y} - D^s_{11}\frac{\partial^2 w_b}{\partial x^2} - D^s_{12}\frac{\partial^2 w_b}{\partial y^2} - H^s_{11}\frac{\partial^2 w_s}{\partial x^2} - H^s_{12}\frac{\partial^2 w_s}{\partial y^2} + Y^s_{13}w_z \quad (9g)$$

$$M^s_y = B^s_{12}\frac{\partial u_0}{\partial x} + B^s_{22}\frac{\partial v_0}{\partial y} - D^s_{12}\frac{\partial^2 w_b}{\partial x^2} - D^s_{22}\frac{\partial^2 w_b}{\partial y^2} - H^s_{12}\frac{\partial^2 w_s}{\partial x^2} - H^s_{22}\frac{\partial^2 w_s}{\partial y^2} + Y^s_{23}w_z \quad (9h)$$

$$M^s_{xy} = B^s_{66}\left(\frac{\partial u_0}{\partial y} + \frac{\partial v_0}{\partial x}\right) - 2D^s_{66}\frac{\partial^2 w_b}{\partial x\partial y} - 2H^s_{66}\frac{\partial^2 w_s}{\partial x\partial y} \quad (9i)$$

$$N_z = X_{13}\frac{\partial u_0}{\partial x} + X_{23}\frac{\partial v_0}{\partial y} - Y_{13}\frac{\partial^2 w_b}{\partial x^2} - Y_{23}\frac{\partial^2 w_b}{\partial y^2} - Y^s_{13}\frac{\partial^2 w_s}{\partial x^2} - Y^s_{23}\frac{\partial^2 w_s}{\partial y^2} + Z_{33}w_z \quad (9j)$$

$$Q_x = A^s_{55}\left(\frac{\partial w_s}{\partial x} + \frac{\partial w_z}{\partial x}\right) \quad (9k)$$

$$Q_y = A^s_{44}\left(\frac{\partial w_s}{\partial y} + \frac{\partial w_z}{\partial y}\right) \quad (9l)$$

$$\left(A_{ij}, A^s_{ij}, B_{ij}, B^s_{ij}, D_{ij}, D^s_{ij}, H^s_{ij}\right) = \int_{-h/2}^{h/2}\left(1, g^2, z, f, z^2, fz, f^2\right)C_{ij}\,dz \quad (9m)$$

$$\left(X_{ij}, Y_{ij}, Y^s_{ij}, Z_{ij}\right) = \int_{-h/2}^{h/2}\left(g', g'z, g'f, g'^2\right)C_{ij}\,dz \quad (9n)$$

The variation of potential energy of the applied loads can be expressed thus

$$\delta V = -\int_A q\left(\delta w_b + \delta w_s + g(z)\delta w_z\right)dA \quad (10)$$

where q is the distributed transverse load. The variation of kinetic energy of the plate can be written in the form

$$\delta K = \int_{-h/2}^{h/2} \int_A (\dot{u}\delta\dot{u} + \dot{v}\delta\dot{v} + \dot{w}\delta\dot{w})\rho(z)dAdz \tag{11}$$

$$\begin{aligned}\delta K = \int_A [& I_0(\dot{u}_0\delta\dot{u}_0 + \dot{v}_0\delta\dot{v}_0 + (\dot{w}_b + \dot{w}_s)(\delta\dot{w}_b + \delta\dot{w}_s)) - I_1(\dot{u}_0\frac{\partial\delta\dot{w}_b}{\partial x} + \frac{\partial\dot{w}_b}{\partial x}\delta\dot{u}_0 + \dot{v}_0\frac{\partial\delta\dot{w}_b}{\partial y} + \frac{\partial\dot{w}_b}{\partial y}\delta\dot{v}_0) \\ & - J_1(\dot{u}_0\frac{\partial\delta\dot{w}_s}{\partial x} + \frac{\partial\dot{w}_s}{\partial x}\delta\dot{u}_0 + \dot{v}_0\frac{\partial\delta\dot{w}_s}{\partial y} + \frac{\partial\dot{w}_s}{\partial y}\delta\dot{v}_0) + I_2(\frac{\partial\dot{w}_b}{\partial x}\frac{\partial\delta\dot{w}_b}{\partial x} + \frac{\partial\dot{w}_b}{\partial y}\frac{\partial\delta\dot{w}_b}{\partial y}) + \\ & + K_2(\frac{\partial\dot{w}_s}{\partial x}\frac{\partial\delta\dot{w}_s}{\partial x} + \frac{\partial\dot{w}_s}{\partial y}\frac{\partial\delta\dot{w}_s}{\partial y}) + J_2(\frac{\partial\dot{w}_b}{\partial x}\frac{\partial\delta\dot{w}_s}{\partial x} + \frac{\partial\dot{w}_s}{\partial x}\frac{\partial\delta\dot{w}_b}{\partial x} + \frac{\partial\dot{w}_b}{\partial y}\frac{\partial\delta\dot{w}_s}{\partial y} + \frac{\partial\dot{w}_s}{\partial y}\frac{\partial\delta\dot{w}_b}{\partial y}) + \\ & + J_1^s((\dot{w}_b + \dot{w}_s)\delta\dot{w}_z + w_z\delta(\dot{w}_b + \dot{w}_s)) + K_2^s\dot{w}_z\delta\dot{w}_z]dA\end{aligned} \tag{12}$$

where the dot-superscript convention corresponds to differentiation with respect to the time variable *t*; and $(I_0, I_1, I_2, J_1^s, J_1, J_2, K_2^s, K_2)$ are mass inertias, defined as follows

$$(I_0, I_1, I_2) = \int_{-h/2}^{h/2} (1, z, z^2)\rho(z).dz \tag{13a}$$

$$(J_1^s, J_1, J_2) = \int_{-h/2}^{h/2} (g(z), f(z), z.f(z))\rho(z).dz \tag{13b}$$

$$(K_2^s, K_2) = \int_{-h/2}^{h/2} (g^2(z), f^2(z))\rho(z).dz \tag{13c}$$

Substituting the expressions for δU; δV, and δK from Eqs. (6), (10), and (12) into Eq. (5) and integrating by parts, and collecting the coefficients of δu_0; δv_0; δw_b; δw_s and δw_z, the following equations of motion of the plate are obtained

$$\delta u_0 : \ \frac{\partial N_x}{\partial x} + \frac{\partial N_{xy}}{\partial y} = I_0\ddot{u}_0 - I_1\frac{\partial\ddot{w}_b}{\partial x} - J_1\frac{\partial\ddot{w}_s}{\partial x} \tag{14a}$$

$$\delta v_0 : \ \frac{\partial N_{xy}}{\partial x} + \frac{\partial N_y}{\partial y} = I_0\ddot{v}_0 - I_1\frac{\partial\ddot{w}_b}{\partial y} - J_1\frac{\partial\ddot{w}_s}{\partial y} \tag{14b}$$

$$\begin{aligned}\delta w_b : \ & \frac{\partial^2 M_x^b}{\partial x^2} + 2\frac{\partial^2 M_{xy}^b}{\partial x\partial y} + \frac{\partial^2 M_y^b}{\partial y^2} + q = I_0(\ddot{w}_b + \ddot{w}_s) + J_1^s\ddot{w}_z + I_1\left(\frac{\partial\ddot{u}_0}{\partial x} + \frac{\partial\ddot{v}_0}{\partial y}\right) - I_2\left(\frac{\partial^2\ddot{w}_b}{\partial x^2} + \frac{\partial^2\ddot{w}_b}{\partial y^2}\right) \\ & - J_2\left(\frac{\partial^2\ddot{w}_s}{\partial x^2} + \frac{\partial^2\ddot{w}_s}{\partial y^2}\right)\end{aligned} \tag{14c}$$

$$\begin{aligned}\delta w_s : \ & \frac{\partial^2 M_x^s}{\partial x^2} + 2\frac{\partial^2 M_{xy}^s}{\partial x\partial y} + \frac{\partial^2 M_y^s}{\partial y^2} + \frac{\partial Q_x}{\partial x} + \frac{\partial Q_y}{\partial y} + q = I_0(\ddot{w}_b + \ddot{w}_s) + J_1^s\ddot{w}_z + J_1\left(\frac{\partial\ddot{u}_0}{\partial x} + \frac{\partial\ddot{v}_0}{\partial y}\right) - J_2\left(\frac{\partial^2\ddot{w}_b}{\partial x^2} + \frac{\partial^2\ddot{w}_b}{\partial y^2}\right) \\ & - K_2\left(\frac{\partial^2\ddot{w}_s}{\partial x^2} + \frac{\partial^2\ddot{w}_s}{\partial y^2}\right)\end{aligned} \tag{14d}$$

$$\delta w_z : \ \frac{\partial Q_x}{\partial x} + \frac{\partial Q_y}{\partial y} - N_z + gq = J_1^s(\ddot{w}_b + \ddot{w}_s) + K_2^s\ddot{w}_z \tag{14e}$$

2.3 Constitutive equations

The material properties of FGM plates are assumed to vary continuously through the thickness. Three homogenization methods are deployable for the computation of the Young's modulus E(z) namely

- The exponential distribution,
- The power law distribution,
- The Mori-Tanaka scheme.

For the exponential distribution, the Young's modulus is given as (Zenkour 2007)

$$E(z) = E_0 e^{P(0.5+z/h)} \tag{15}$$

where E_0 is the Young's modulus of the homogeneous plate; E_m=E_0 and E_c=$E_0 e^{p}$ denote Young's modulus of the bottom (metal) and top (ceramic) surfaces of the FGM plate, respectively; E_0 is Young's modulus of the homogeneous plate; and p is a parameter that indicates the material variation through the plate thickness. For the power law distribution, the Young's modulus is given as (Reddy 2000)

$$E(z) = E_m + (E_c - E_m)(\frac{1}{2} + \frac{z}{h})^P \tag{16}$$

For Mori-Tanaka scheme, the Young's modulus is given as (Mori Tanaka 1973)

$$E(z) = E_m + (E_c - E_m)(\frac{(\frac{1}{2} + \frac{z}{h})^P}{1 + (1 - (\frac{1}{2} + \frac{z}{h})^P)(\frac{E_c}{E_m} - 1)\frac{(1+\nu)}{3-3\nu}}) \tag{17}$$

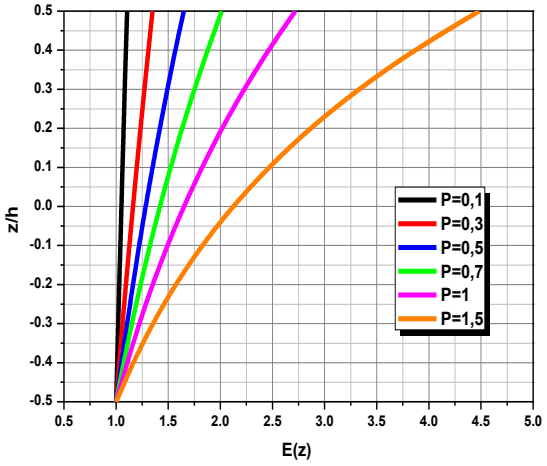

Fig. 2 The exponential distribution of the Young's modulus E(z) along the thickness of an E-FGM plate

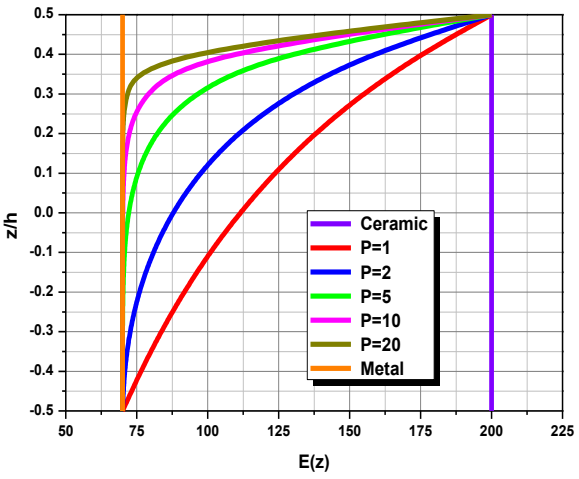

Fig. 3 The distribution of the Young's modulus E(z) along the thickness of an FGM plate according to Mori-Tanaka scheme

The linear constitutive relations of a FG plate can be written as

$$\begin{Bmatrix} \sigma_x \\ \sigma_y \\ \sigma_z \\ \sigma_{yz} \\ \sigma_{xz} \\ \sigma_{xy} \end{Bmatrix} = \begin{bmatrix} C_{11} & C_{12} & C_{13} & 0 & 0 & 0 \\ C_{12} & C_{22} & C_{23} & 0 & 0 & 0 \\ C_{13} & C_{23} & C_{33} & 0 & 0 & 0 \\ 0 & 0 & 0 & C_{44} & 0 & 0 \\ 0 & 0 & 0 & 0 & C_{55} & 0 \\ 0 & 0 & 0 & 0 & 0 & C_{66} \end{bmatrix} \begin{Bmatrix} \varepsilon_x \\ \varepsilon_y \\ \varepsilon_z \\ \gamma_{yz} \\ \gamma_{xz} \\ \gamma_{xy} \end{Bmatrix} \tag{18}$$

where (σ_x, σ_y, σ_z, τ_{yz}, τ_{xz}, τ_{xy}) and (ε_x, ε_y, ε_z, γ_{yz}, γ_{xz}, γ_{xy}) are the stress and strain components, respectively. The computation of the elastic constants C_{ij} depends on which assumption of ε_z we consider. If ε_z=0, then C_{ij} are the plane stress reduced elastic constants, defined as

$$C_{11} = C_{22} = \frac{E(z)}{(1-\nu^2)} \tag{19a}$$

$$C_{12} = \nu C_{11} \tag{19b}$$

$$C_{44} = C_{55} = C_{66} = \frac{E(z)}{2(1+\nu)} \tag{19c}$$

If $\varepsilon_z \neq 0$ (thickness stretching), then C_{ij} are the three-dimensional elastic constants, given by

$$C_{11} = C_{22} = C_{33} = \frac{(1-\nu)E(z)}{(1-2\nu)(1+\nu)} \tag{20a}$$

$$C_{12} = C_{13} = C_{23} = \frac{E(z)}{(1-2\nu)(1+\nu)} \tag{20b}$$

$$C_{44} = C_{55} = C_{66} = \frac{E(z)}{2(1+\nu)} \tag{20c}$$

Lamé's coefficients are: $$\lambda(z) = \frac{\nu E(z)}{(1-2\nu)(1+\nu)} \tag{21a}$$

$$\mu(z) = G(z) = \frac{E(z)}{2(1+\nu)} \tag{21b}$$

The module $E(z)$, $G(z)$ and the elastic coefficients C_{ij} vary through the thickness according to Eqs. (15), (16) or (17). By substituting Eq. (4) into Eq. (18) and the subsequent results into Eq. (8), the stress resultants are readily obtained as

$$\begin{Bmatrix} N \\ M^b \\ M^s \end{Bmatrix} = \begin{bmatrix} A & B & B^s \\ A & D & D^s \\ B^s & D^s & H^s \end{bmatrix} \begin{Bmatrix} \varepsilon \\ k^b \\ k^s \end{Bmatrix} + \begin{Bmatrix} L \\ L^a \\ R \end{Bmatrix} \varepsilon_z^0 \tag{22a}$$

$$S = A^s \gamma \tag{22b}$$

$$N_z = R^a w_z + L(\varepsilon_x^0 + \varepsilon_y^0) + L^a (k_x^b + k_y^b) + R(k_x^s + k_y^s) \tag{22c}$$

where

$$N = \{N_x, N_y, N_{xy}\}, \quad M^b = \{M_x^b, M_y^b, M_{xy}^b\}, \quad M^s = \{M_x^s, M_y^s, M_{xy}^s\}, \tag{23a}$$

$$\varepsilon = \{\varepsilon_x^0, \varepsilon_y^0, \gamma_{xy}^0\}, \quad k^b = \{k_x^b, k_y^b, k_{xy}^b\}, \quad k^s = \{k_x^s, k_y^s, k_{xy}^s\}, \tag{23b}$$

$$\boldsymbol{A} = \begin{bmatrix} \boldsymbol{A}_{11} & \boldsymbol{A}_{12} & 0 \\ \boldsymbol{A}_{12} & \boldsymbol{A}_{22} & 0 \\ 0 & 0 & \boldsymbol{A}_{66} \end{bmatrix}, \quad \boldsymbol{B} = \begin{bmatrix} \boldsymbol{B}_{11} & \boldsymbol{B}_{12} & 0 \\ \boldsymbol{B}_{12} & \boldsymbol{B}_{22} & 0 \\ 0 & 0 & \boldsymbol{B}_{66} \end{bmatrix}, \quad \boldsymbol{D} = \begin{bmatrix} \boldsymbol{D}_{11} & \boldsymbol{D}_{12} & 0 \\ \boldsymbol{D}_{12} & \boldsymbol{D}_{22} & 0 \\ 0 & 0 & \boldsymbol{D}_{66} \end{bmatrix}, \tag{23c}$$

$$\boldsymbol{B^s} = \begin{bmatrix} \boldsymbol{B}_{11}^{\boldsymbol{s}} & \boldsymbol{B}_{12}^{\boldsymbol{s}} & 0 \\ \boldsymbol{B}_{12}^{\boldsymbol{s}} & \boldsymbol{B}_{22}^{\boldsymbol{s}} & 0 \\ 0 & 0 & \boldsymbol{B}_{66}^{\boldsymbol{s}} \end{bmatrix}, \quad \boldsymbol{D^s} = \begin{bmatrix} \boldsymbol{D}_{11}^{\boldsymbol{s}} & \boldsymbol{D}_{12}^{\boldsymbol{s}} & 0 \\ \boldsymbol{D}_{12}^{\boldsymbol{s}} & \boldsymbol{D}_{22}^{\boldsymbol{s}} & 0 \\ 0 & 0 & \boldsymbol{D}_{66}^{\boldsymbol{s}} \end{bmatrix}, \quad \boldsymbol{H^s} = \begin{bmatrix} \boldsymbol{H}_{11}^{\boldsymbol{s}} & \boldsymbol{H}_{12}^{\boldsymbol{s}} & 0 \\ \boldsymbol{H}_{12}^{\boldsymbol{s}} & \boldsymbol{H}_{22}^{\boldsymbol{s}} & 0 \\ 0 & 0 & \boldsymbol{H}_{66}^{\boldsymbol{s}} \end{bmatrix} \tag{23d}$$

,

$$S = \{S_{xz}^s, S_{yz}^s\}, \qquad \gamma = \{\gamma_{xz}, \gamma_{yz}\}, \qquad A^s = \begin{bmatrix} A_{44}^s & 0 \\ 0 & A_{55}^s \end{bmatrix}, \tag{23e}$$

$$\begin{Bmatrix} \boldsymbol{L} \\ \boldsymbol{L}^a \\ \boldsymbol{R} \\ \boldsymbol{R}^a \end{Bmatrix} = \int_{-h/2}^{h/2} \lambda(z) \begin{Bmatrix} \boldsymbol{1} \\ \boldsymbol{z} \\ \boldsymbol{f(z)} \\ \boldsymbol{g'(z)} \dfrac{\boldsymbol{1-\nu}}{\boldsymbol{\nu}} \end{Bmatrix} \boldsymbol{g'(z)} dz \tag{23f}$$

where A_{ij}, B_{ij}, etc., are the plate stiffness, defined by

$$\begin{Bmatrix} A_{11} & B_{11} & D_{11} & B_{11}^s & D_{11}^s & H_{11}^s \\ A_{12} & B_{12} & D_{12} & B_{12}^s & D_{12}^s & H_{12}^s \\ A_{66} & B_{66} & D_{66} & B_{66}^s & D_{66}^s & H_{66}^s \end{Bmatrix} = \int_{-h/2}^{h/2} \lambda(z) \left(1, z, z^2, f(z), z\, f(z), f^2(z)\right) \begin{Bmatrix} \dfrac{1-\nu}{\nu} \\ 1 \\ \dfrac{1-2\nu}{2\nu} \end{Bmatrix} dz, \tag{24a}$$

and:
$$\left(A_{22}, B_{22}, D_{22}, B^s_{22}, D^s_{22}, H^s_{22}\right)=\left(A_{11}, B_{11}, D_{11}, B^s_{11}, D^s_{11}, H^s_{11}\right) \tag{24b}$$

$$A^s_{44}=A^s_{55}=\int_{-h/2}^{h/2}\mu(z)(g(z))^2\,dz, \tag{24c}$$

2.4 Equations of motion in terms of displacements

Introducing Eq. (23) into Eq. (14), the equations of motion can be expressed in terms of displacements (δu_0; δv_0; δw_b; δw_s and δw_z) and the appropriate equations take the form

$$A_{11}\frac{\partial^2 u_0}{\partial x^2}+A_{66}\frac{\partial^2 u_0}{\partial y^2}+(A_{12}+A_{66})\frac{\partial^2 v_0}{\partial x\partial y}-B_{11}\frac{\partial^3 w_b}{\partial x^3}-(B_{12}+2B_{66})\frac{\partial^3 w_b}{\partial x\partial y^2}-(B^s_{12}+2B^s_{66})\frac{\partial^3 w_s}{\partial x\partial y^2}$$
$$-B^s_{11}\frac{\partial^3 w_s}{\partial x^3}+X_{13}\frac{\partial w_z}{\partial x}=I_0\ddot{u}_0-I_1\frac{\partial\ddot{w}_b}{\partial x}-J_1\frac{\partial\ddot{w}_s}{\partial x} \tag{25a}$$

$$A_{22}\frac{\partial^2 v_0}{\partial y^2}+A_{66}\frac{\partial^2 v_0}{\partial x^2}+(A_{12}+A_{66})\frac{\partial^2 u_0}{\partial x\partial y}-B_{22}\frac{\partial^3 w_b}{\partial y^3}-(B_{12}+2B_{66})\frac{\partial^3 w_b}{\partial x^2\partial y}-(B^s_{12}+2B^s_{66})\frac{\partial^3 w_s}{\partial x^2\partial y}$$
$$-B^s_{22}\frac{\partial^3 w_s}{\partial y^3}+X_{23}\frac{\partial w_z}{\partial y}=I_0\ddot{v}_0-I_1\frac{\partial\ddot{w}_b}{\partial y}-J_1\frac{\partial\ddot{w}_s}{\partial y} \tag{25b}$$

$$B_{11}\frac{\partial^3 u_0}{\partial x^3}+(B_{12}+2B_{66})\frac{\partial^3 u_0}{\partial x\partial y^2}+(B_{12}+2B_{66})\frac{\partial^3 v_0}{\partial x^2\partial y}+B_{22}\frac{\partial^3 v_0}{\partial y^3}-D_{11}\frac{\partial^4 w_b}{\partial x^4}$$
$$-2(D_{12}+2D_{66})\frac{\partial^4 w_b}{\partial x^2\partial y^2}-D_{22}\frac{\partial^4 w_b}{\partial y^4}-D^s_{11}\frac{\partial^4 w_s}{\partial x^4}-2(D^s_{12}+2D^s_{66})\frac{\partial^4 w_s}{\partial x^2\partial y^2}-D^s_{22}\frac{\partial^4 w_s}{\partial y^4}$$
$$+Y_{13}\frac{\partial^2 w_z}{\partial x^2}+Y_{23}\frac{\partial^2 w_z}{\partial y^2}+q=I_0(\ddot{w}_b+\ddot{w}_s)+J^s_1\ddot{w}_z+J_1\left(\frac{\partial\ddot{u}_0}{\partial x}+\frac{\partial\ddot{v}_0}{\partial y}\right)-I_2\left(\frac{\partial^2\ddot{w}_b}{\partial x^2}+\frac{\partial^2\ddot{w}_b}{\partial y^2}\right) \tag{25c}$$
$$-J_2\left(\frac{\partial^2\ddot{w}_s}{\partial x^2}+\frac{\partial^2\ddot{w}_s}{\partial y^2}\right)$$

$$B^s_{11}\frac{\partial^3 u_0}{\partial x^3}+(B^s_{12}+2B^s_{66})\frac{\partial^3 u_0}{\partial x\partial y^2}+(B^s_{12}+2B^s_{66})\frac{\partial^3 v_0}{\partial x^2\partial y}+B^s_{22}\frac{\partial^3 v_0}{\partial y^3}-D^s_{11}\frac{\partial^4 w_b}{\partial x^4}$$
$$-2(D^s_{12}+2D^s_{66})\frac{\partial^4 w_b}{\partial x^2\partial y^2}-D^s_{22}\frac{\partial^4 w_b}{\partial y^4}-H^s_{11}\frac{\partial^4 w_s}{\partial x^4}-2(H^s_{12}+2H^s_{66})\frac{\partial^4 w_s}{\partial x^2\partial y^2}$$
$$-H^s_{22}\frac{\partial^4 w_s}{\partial y^4}+A^s_{55}\frac{\partial^2 w_s}{\partial x^2}+A^s_{44}\frac{\partial^2 w_s}{\partial y^2}+(Y^s_{13}+A^s_{55})\frac{\partial^2 w_z}{\partial x^2}+(Y^s_{23}+A^s_{44})\frac{\partial^2 w_z}{\partial y^2}+q= \tag{25d}$$
$$I_0(\ddot{w}_b+\ddot{w}_s)+J^s_1\ddot{w}_z+J_1\left(\frac{\partial\ddot{u}_0}{\partial x}+\frac{\partial\ddot{v}_0}{\partial y}\right)-J_2\left(\frac{\partial^2\ddot{w}_b}{\partial x^2}+\frac{\partial^2\ddot{w}_b}{\partial y^2}\right)-K_2\left(\frac{\partial^2\ddot{w}_s}{\partial x^2}+\frac{\partial^2\ddot{w}_s}{\partial y^2}\right)$$

$$-X_{13}\frac{\partial u_0}{\partial x}-X_{23}\frac{\partial v_0}{\partial y}+Y_{13}\frac{\partial^2 w_b}{\partial x^2}+Y_{23}\frac{\partial^2 w_b}{\partial y^2}+(Y^s_{13}+A^s_{55})\frac{\partial^2 w_s}{\partial x^2}+(Y^s_{23}+A^s_{44})\frac{\partial^2 w_s}{\partial y^2}$$
$$+A^s_{55}\frac{\partial^2 w_z}{\partial x^2}+A^s_{44}\frac{\partial^2 w_z}{\partial y^2}-Z_{33}w_z+gq=J^s_1(\ddot{w}_b+\ddot{w}_s)+K^s_2\ddot{w}_z \tag{25e}$$

2.5 Analytical solutions

Consider a simply supported rectangular plate with length a and width *b* under transverse load *q*. Based on Navier solution method, the following expansions of displacements (u_0; v_0; w_b; w_s; w_z) are assumed as

$$\begin{aligned}
u_0(x,y) &= \sum_{m=1}^{\infty}\sum_{n=1}^{\infty} U_{mn} e^{i\omega t}\cos(\lambda x)\sin(\mu y)\\
v_0(x,y) &= \sum_{m=1}^{\infty}\sum_{n=1}^{\infty} V_{mn} e^{i\omega t}\sin(\lambda x)\cos(\mu y)\\
w_b(x,y) &= \sum_{m=1}^{\infty}\sum_{n=1}^{\infty} W_{bmn} e^{i\omega t}\sin(\lambda x)\sin(\mu y)\\
w_s(x,y) &= \sum_{m=1}^{\infty}\sum_{n=1}^{\infty} W_{smn} e^{i\omega t}\sin(\lambda x)\sin(\mu y)\\
w_z(x,y) &= \sum_{m=1}^{\infty}\sum_{n=1}^{\infty} W_{zmn} e^{i\omega t}\sin(\lambda x)\sin(\mu y)
\end{aligned} \tag{26}$$

where U_{mn}, V_{mn}, W_{bmn}, W_{smn} and W_{zmn} unknown parameters must be determined, ω is the Eigen frequency associated with (m, n) the Eigen-mode, and $\lambda = \frac{m\pi}{a}$ and $\mu = \frac{n\pi}{b}$.

The transverse load *q* is also expanded in the double-Fourier sine series as follows

$$q(x,y) = \sum_{m=1}^{\infty}\sum_{n=1}^{\infty} Q_{mn}\sin(\lambda x)\sin(\mu y) \tag{27}$$

The coefficients Q_{mn} are given below for some typical loads

$$Q_{mn} = \frac{4}{ab}\int_0^a\int_0^b q(x,y)\sin(\lambda x)\sin(\mu y)dxdy \tag{28}$$

$$\begin{cases} Q_{mn} = q_0 \\ Q_{mn} = \dfrac{16q_0}{mn\pi^2} \end{cases}$$

$$\left(\begin{bmatrix} a_{11} & a_{12} & a_{13} & a_{14} & a_{15}\\ a_{12} & a_{22} & a_{23} & a_{24} & a_{25}\\ a_{13} & a_{23} & a_{33} & a_{34} & a_{35}\\ a_{14} & a_{24} & a_{34} & a_{44} & a_{45}\\ a_{15} & a_{25} & a_{35} & a_{45} & a_{55} \end{bmatrix} - \omega^2 \begin{bmatrix} m_{11} & 0 & m_{13} & m_{14} & 0\\ 0 & m_{22} & m_{23} & m_{24} & 0\\ m_{13} & m_{23} & m_{33} & m_{34} & m_{35}\\ m_{14} & m_{24} & m_{34} & m_{44} & m_{45}\\ 0 & 0 & m_{35} & m_{45} & m_{55} \end{bmatrix}\right)\begin{Bmatrix} U_{mn}\\ V_{mn}\\ W_{bmn}\\ W_{smn}\\ W_{zmn}\end{Bmatrix} = \begin{Bmatrix} 0\\ 0\\ Q_{mn}\\ Q_{mn}\\ 0\end{Bmatrix} \tag{29}$$

Where

$$\begin{aligned}
a_{11} &= A_{11}\lambda^2 + A_{66}\mu^2 \qquad a_{13} = -\lambda[B_{11}\lambda^2 + (B_{12}+2B_{66})\mu^2]\\
a_{12} &= \lambda\mu(A_{12}+A_{66})\\
a_{14} &= -\lambda[B^s_{11}\lambda^2 + (B^s_{12}+2B^s_{66})\mu^2]\\
a_{15} &= X_{13}\lambda \qquad\qquad a_{23} = -\mu[B_{22}\mu^2 + (B_{12}+2B_{66})\lambda^2]
\end{aligned} \tag{30}$$

$$a_{22} = A_{66}\lambda^2 + A_{22}\mu^2 \qquad a_{24} = -\mu[B^s_{22}\mu^2 + (B^s_{12} + 2B^s_{66})\lambda^2]$$

$$a_{25} = X_{23}\mu \qquad a_{33} = D_{11}\lambda^4 + 2(D_{12} + 2D_{66})\lambda^2\mu^2 + D_{22}\mu^4$$

$$a_{35} = Y_{13}\lambda^2 + Y_{23}\mu^2 \qquad a_{34} = D^s_{11}\lambda^4 + 2(D^s_{12} + 2D^s_{66})\lambda^2\mu^2 + D^s_{22}\mu^4$$

$$a_{55} = A^s_{55}\lambda^2 + A^s_{44}\mu^2 + Z_{33} \qquad a_{45} = (Y^s_{13} + A^s_{55})\lambda^2 + (Y^s_{23} + A^s_{44})\mu^2$$

$$a_{44} = H^s_{11}\lambda^4 + 2(H^s_{12} + 2H^s_{66})\lambda^2\mu^2 + H^s_{22}\mu^4 + A^s_{55}\lambda^2 + A^s_{44}\mu^2$$

$$m_{11} = I_0 \qquad m_{13} = -\lambda I_1 \qquad m_{14} = -\lambda J_1 \qquad m_{22} = I_0 \qquad m_{23} = -\mu I_1$$

$$m_{24} = -\mu J_1 \qquad m_{33} = I_0 + I_2(\lambda^2 + \mu^2) \qquad m_{35} = J_0$$

$$m_{34} = I_0 + J_1(\lambda^2 + \mu^2) \qquad m_{44} = I_0 + K_2(\lambda^2 + \mu^2) \qquad m_{45} = J_0 \qquad m_{55} = K_0$$

3. Numerical results and discussions

In this study, various numerical examples are presented and discussed to verify the accuracy of the present theory in predicting the natural frequency of simply supported plates. For verification purpose; the obtained results are compared with exact solutions of 3D elasticity theory and those predicted by quasi-3D (Zenkour 2007, Mantari 2012) theories and HSDT (Hassaine Daouadji 2013). The type of FGM plates are used in this study, and their corresponding material properties are:

- Metal Aluminum Al: $E_m = 70GPa$; $\nu = 0.3$, $\rho_m = 2702kg/m^3$
- Ceramic : Alumina Al_2O_3: $E_c = 380GPa$; $\nu = 0.3$, $\rho = 3800kg/m^3{}_c$
- Ceramic : Zirconia ZrO_2: $E_c = 200GPa$; $\nu = 0.3$, $\rho_c = 5700kg/m^3$

The description of various theories is given in Table 1. Quasi-3D (Zenkour 2007, Mantari 2012) theory is the HSDT (Hassaine Daouadji 2013) with a higher-order variation for the transverse displacement ($\varepsilon_z \neq 0$). The difference among quasi-3D theories comes from the use of shear strain shape functions. For example, the quasi-3D theory is based on trigonometric functions for both in-plane and transverse displacements, while the quasi-3D theory (Mantari 2012) is based on cubic function for the in-plane displacement and parabolic function for the transverse displacement. The results of the present model are also computed independently in this work using Eq. (29). For bending analysis, a plate subjected to a sinusoidal load is considered, for convenience, the following dimensionless forms are used

$$\bar{z} = z/h, \quad \bar{u} = \frac{10E_c h^3}{a^4 q_0}\left(0, \frac{b}{2}, z\right), \quad \bar{v} = \frac{10E_c h^3}{a^4 q_0}\left(\frac{a}{2}, 0, z\right),$$

$$\bar{w} = \frac{10E_c h^3}{a^4 q_0} w\left(\frac{a}{2}, \frac{b}{2}, z\right), \quad \bar{\sigma}_x = \frac{h}{a.q_0}\sigma_x\left(\frac{a}{2}, \frac{b}{2}, z\right), \quad \bar{\tau}_{xy} = \frac{h}{a.q_0}\tau_{xy}(0,0,z),$$

$$\bar{\tau}_{xz} = \frac{h}{a.q_0}\tau_{xz}\left(0, \frac{b}{2}, z\right), \quad \bar{\tau}_{yz} = \frac{h}{a.q_0}\tau_{xz}\left(\frac{a}{2}, 0, z\right) \quad \widehat{\omega} = \omega.h\sqrt{\frac{\rho_c}{E_c}},$$

$$\bar{\omega} = \omega.\frac{a^2}{h}\sqrt{\frac{\rho_m}{E_m}},$$

Table 1 Displacement models

Model	Theory	ε_z	Unknown
Present Model	Quasi -3D with trigonometric functions	$\varepsilon_z \neq 0$	5
HSDT (Hassaine Daouadji 2013)	Higher order Shear Deformation Theory	$\varepsilon_z = 0$	4
Quasi-3D (Neves 2012)	Quasi-3D theory with hyperbolic and parabolic functions	$\varepsilon_z \neq 0$	9
Quasi-3D (Neves 2013)	Quasi-3D theory with cubic and parabolic functions	$\varepsilon_z \neq 0$	9
Quasi-3D (Zenkour 2007)	Quasi-3D theory with sinusoidal functions	$\varepsilon_z \neq 0$	6
Quasi-3D (Mantari 2012)	Quasi-3D theory with sinusoidal functions	$\varepsilon_z \neq 0$	6

3.1 Numerical results for bending analysis

Numerical results for bending analysis, an exponentially graded plate subjected to sinusoidal loads is considered. The effective Young's modulus is calculated using the exponential distribution (Zenkour 2007) in Eq. (15) and the power law distribution (Reddy 2000) in Eq. (16). Tables 2-9 contain dimensionless displacements and stresses for rectangular plates with various values of aspect ratio b/a, thickness ratio a/h, and material parameter P. The obtained results are compared with exact 3D solutions (Zenkour 2007) and those predicted by quasi-3D theories (Zenkour 2007, Thai 2013, Mantari 2012), HSDT (Hassaine Daouadji 2013), and present model (Quasi -3D with trigonometric functions). It is noted that the exact 3D solutions (Zenkour 2007) are not available for a/h=10. It is observed that the present model and quasi-3D theories give solutions close to each other, and their solutions are in an excellent agreement with the exact 3D solutions. Inspection of Tables 2-9 demonstrates that the present computations are in very good agreement with quasi-3-dimensional solutions available in the literature.

Figs. 4-11 illustrates the distribution of displacements, deflection and stresses across the thickness of thick plates. The results presented demonstrate that the same accuracy is achievable with the present theory using a lower number of unknowns than other theories, and clearly highlights how the present theory is simpler and more easily deployed in FGM structural mechanics simulations. Again, an excellent agreement between the results is seen. Thus, the proposed quasi-3D trigonometric higher order shear and normal deformation theory is not only accurate but also simple in predicting the behavior of FGM plates.

Table 2 Dimensionless transverse deflection $\overline{w}$ of plates (a/h=2)

b/a	Theory	P					
		0.1	0.3	0.5	0.7	1.0	1.5
3	Present Model	1.4422	1.3038	1.1777	1.0629	0.9098	0.6993
	3D (Zenkour 2007)	1.4430	1.3116	1.1913	1.0812	0.9334	0.7275
	Quasi-3D (Zenkour 2006)	1.4421	1.3037	1.1776	1.0628	0.9104	0.6993
	Quasi-3D (Mantari 2012)	1.4419	1.3035	1.1774	1.0626	0.9096	0.6991
	HSDT (Hassaine Daouadji 2013)	1.5341	1.3874	1.2541	1.1330	0.9719	0.7506
2	Present Model	1.1942	1.0796	0.9751	0.8800	0.7532	0.5786

Table 2 Continued

b/a	Theory	P					
		0.1	0.3	0.5	0.7	1.0	1.5
2	3D (Zenkour 2007)	1.1945	1.0859	0.9864	0.8952	0.7727	0.6017
	Quasi-3D (Zenkour 2006)	1.1941	1.0795	0.9750	0.8799	0.7538	0.5786
	Quasi-3D (Mantari 2012)	1.1938	1.0793	0.9748	0.8797	0.7530	0.5785
	HSDT (Hassaine Daouadji 2013)	1.2777	1.1554	1.0442	0.9431	0.8086	0.6238
1	Present Model	0.5780	0.5225	0.4719	0.4258	0.3642	0.2794
	3D (Zenkour 2007)	0.5769	0.5247	0.4766	0.4324	0.3727	0.2890
	Quasi-3D (Zenkour 2006)	0.5779	0.5224	0.4718	0.4257	0.3649	0.2794
	Quasi-3D (Mantari 2012)	0.5776	0.5222	0.4716	0.4255	0.3640	0.2792
	HSDT (Hassaine Daouadji 2013)	0.6363	0.5752	0.5195	0.4688	0.4011	0.3079

Table 3 Dimensionless transverse deflection $\overline{w}$ of plates (a/h=4)

b/a	Theory	P					
		0.1	0.3	0.5	0.7	1.0	1.5
3	Present Model	1.0124	0.9155	0.8272	0.7470	0.6404	0.4941
	3D (Zenkour 2007)	1.0134	0.9190	0.8335	0.7561	0.6533	0.5121
	Quasi-3D (Zenkour 2006)	1.0094	0.9127	0.8248	0.7449	0.6385	0.4927
	Quasi-3D (Mantari 2012)	1.0124	0.9155	0.8272	0.7470	0.6404	0.4941
	HSDT (Hassaine Daouadji 2013)	1.0325	0.9345	0.8459	0.7659	0.6601	0.5154
2	Present Model	0.8145	0.7365	0.6655	0.6009	0.5151	0.3973
	3D (Zenkour 2007)	0.8153	0.7395	0.6707	0.6085	0.5257	0.4120
	Quasi-3D (Mantari 2012)	0.8120	0.7343	0.6635	0.5992	0.5136	0.3962
	HSDT (Hassaine Daouadji 2013)	0.8325	0.7534	0.6819	0.6173	0.5319	0.4150
1	Present Model	0.3486	0.3152	0.2848	0.2571	0.2203	0.1697
	3D (Zenkour 2007)	0.3490	0.3167	0.2875	0.2608	0.2253	0.1805
	Quasi-3D (Zenkour 2006)	0.3475	0.3142	0.2839	0.2563	0.2196	0.1692
	Quasi-3D (Mantari 2012)	0.3486	0.3152	0.2848	0.2571	0.2203	0.1697
	HSDT (Hassaine Daouadji 2013)	0.3602	0.3259	0.2949	0.2668	0.2295	0.1785

Table 4 Dimensionless transverse deflection $\overline{w}$ of plates (a/h=10)

b/a	Theory	P					
		0.1	0.3	0.5	0.7	1.0	1.5
3	Present Model	0.8877	0.8027	0.7255	0.6554	0.5622	0.4346
	Quasi-3D (Mantari 2012)	0.8877	0.8027	0.7255	0.6554	0.5622	0.4346
	HSDT (Hassaine Daouadji 2013)	0.8909	0.8066	0.7307	0.6622	0.5720	0.4489
2	Present Model	0.7037	0.6364	0.5752	0.5196	0.4457	0.3445
	Quasi-3D (Mantari 2012)	0.7037	0.6364	0.5752	0.5196	0.4457	0.3445
	HSDT (Hassaine Daouadji 2013)	0.7066	0.6397	0.5795	0.5252	0.4536	0.3560

Table 4 Continued

b/a	Theory	P					
		0.1	0.3	0.5	0.7	1.0	1.5
1	Present Model	0.2799	0.2531	0.2287	0.2066	0.1772	0.1370
	Quasi-3D (Mantari 2012)	0.2799	0.2531	0.2287	0.2066	0.1772	0.1370
	HSDT (Hassaine Daouadji 2013)	0.2816	0.2550	0.2309	0.2093	0.1807	0.1417

Table 5 Dimensionless in-plane normal stress $\bar{\sigma}_y(h/2)$ of plates (a/h=2)

b/a	Theory	P					
		0.1	0.3	0.5	0.7	1.0	1.5
3	Present Model	0.2909	0.3114	0.3333	0.3567	0.3947	0.4668
	3D (Zenkour 2007)	0.3081	0.3252	0.3436	0.3633	0.3953	0.4562
	Quasi-3D (Zenkour 2006)	0.3042	0.3261	0.3493	0.3741	0.4143	0.4904
	Quasi-3D (Mantari 2012)	0.2920	0.3127	0.3347	0.3582	0.3963	0.4688
	HSDT (Hassaine Daouadji 2013)	0.2366	0.2538	0.2719	0.2912	0.3225	0.3811
2	Present Model	0.3040	0.3259	0.3492	0.3740	0.4142	0.4901
	3D (Zenkour 2007)	0.3200	0.3385	0.3583	0.3796	0.4142	0.4799
	Quasi-3D (Zenkour 2006)	0.3146	0.3376	0.3620	0.3880	0.4300	0.5092
	Quasi-3D (Mantari 2012)	0.3049	0.3269	0.3503	0.3752	0.4155	0.4918
	HSDT (Hassaine Daouadji 2013)	0.2537	0.2722	0.2918	0.3126	0.3462	0.4094
1	Present Model	0.2924	0.3146	0.3382	0.3632	0.4034	0.4783
	3D (Zenkour 2007)	0.3103	0.3292	0.3495	0.3713	0.4067	0.4741
	Quasi-3D (Zenkour 2006)	0.2955	0.3181	0.3421	0.3675	0.4085	0.4851
	Quasi-3D (Mantari 2012)	0.2927	0.3149	0.3385	0.3636	0.4039	0.4790
	HSDT (Hassaine Daouadji 2013)	0.2520	0.2708	0.2908	0.3120	0.3463	0.4106

Table 6 Dimensionless in-plane normal stress $\bar{\sigma}_y(h/2)$ of plates (a/h=4)

b/a	Theory	P					
		0.1	0.3	0.5	0.7	1.0	1.5
3	Present Model	0.2267	0.2408	0.2560	0.2725	0.2997	0.3532
	3D (Zenkour 2007)	0.2319	0.2469	0.2629	0.2800	0.3077	0.3602
	Quasi-3D (Zenkour 2006)	0.2493	0.2656	0.2831	0.3017	0.3323	0.3911
	Quasi-3D (Mantari 2012)	0.2286	0.2429	0.2583	0.2749	0.3024	0.3563
	HSDT (Hassaine Daouadji 2013)	0.2162	0.2312	0.2472	0.2642	0.2916	0.3434
2	Present Model	0.2391	0.2545	0.2710	0.2888	0.3181	0.3749
	3D (Zenkour 2007)	0.2431	0.2591	0.2762	0.2943	0.3238	0.3797
	Quasi-3D (Zenkour 2006)	0.2588	0.2761	0.2946	0.3143	0.3464	0.4079
	Quasi-3D (Mantari 2012)	0.2407	0.2563	0.2730	0.2909	0.3204	0.3776
	HSDT (Hassaine Daouadji 2013)	0.2294	0.2454	0.2624	0.2804	0.3097	0.3647
1	Present Model	0.2235	0.2388	0.2551	0.2726	0.3010	0.3551

Table 6 Continued

b/a	Theory	P					
		0.1	0.3	0.5	0.7	1.0	1.5
1	3D (Zenkour 2007)	0.2247	0.2399	0.2562	0.2736	0.3018	0.3588
	Quasi-3D (Zenkour 2006)	0.2346	0.2510	0.2684	0.2870	0.3171	0.3739
	Quasi-3D (Mantari 2012)	0.2244	0.2398	0.2563	0.2738	0.3024	0.3567
	HSDT (Hassaine Daouadji 2013)	0.2163	0.2316	0.2477	0.2649	0.2927	0.3451

Table 7 Dimensionless in-plane normal stress $\bar{\sigma}_y(h/2)$ of plates (a/h=10)

b/a	Theory	P					
		0.1	0.3	0.5	0.7	1.0	1.5
3	Present Model	0.2094	0.2218	0.2352	0.2497	0.2740	0.3224
	Quasi-3D (Mantari 2012)	0.2115	0.2240	0.2377	0.2524	0.2770	0.3258
	HSDT (Hassaine Daouadji 2013)	0.2104	0.2248	0.2402	0.2565	0.2829	0.3328
2	Present Model	0.2218	0.2354	0.2501	0.2660	0.2923	0.3439
	Quasi-3D (Mantari 2012)	0.2236	0.2375	0.2523	0.2684	0.2950	0.3470
	HSDT (Hassaine Daouadji 2013)	0.2225	0.2378	0.2541	0.2713	0.2993	0.3521
1	Present Model	0.2060	0.2195	0.2340	0.2495	0.2749	0.3235
	Quasi-3D (Mantari 2012)	0.2071	0.2208	0.2354	0.2510	0.2765	0.3253
	HSDT (Hassaine Daouadji 2013)	0.2062	0.2204	0.2355	0.2515	0.2774	0.3264

Table 8 Dimensionless in-plane normal stress $\bar{\sigma}_x(h/2)$ of plates (a/h=10)

b/a	Theory	P					
		0.1	0.3	0.5	0.7	1.0	1.5
3	Present Model	0.5270	0.5629	0.6011	0.6418	0.7077	0.8326
	Quasi-3D (Mantari 2012)	0.5291	0.5652	0.6036	0.6445	0.7107	0.8361
	HSDT (Hassaine Daouadji 2013)	0.5288	0.5651	0.6037	0.6447	0.7112	0.8365
2	Present Model	0.4335	0.4628	0.4941	0.5274	0.5815	0.6841
	Quasi-3D (Mantari 2012)	0.4354	0.4649	0.4963	0.5298	0.5841	0.6871
	HSDT (Hassaine Daouadji 2013)	0.4350	0.4649	0.4966	0.5303	0.5850	0.6881
1	Present Model	0.2060	0.2195	0.2340	0.2495	0.2749	0.3235
	Quasi-3D (Mantari 2012)	0.2071	0.2208	0.2354	0.2510	0.2765	0.3253
	HSDT (Hassaine Daouadji 2013)	0.2062	0.2204	0.2355	0.2515	0.2774	0.3264

Table 9 Dimensionless in-plane normal stress $\bar{\sigma}_{xz}(0)$ of plates (a/h=10)

b/a	Theory	P					
		0.1	0.3	0.5	0.7	1.0	1.5
3	Present Model	0.4283	0.4276	0.4261	0.4239	0.4193	0.4082
	Quasi-3D (Mantari 2012)	0.4295	0.4287	0.4272	0.4251	0.4204	0.4093
	HSDT (Hassaine Daouadji 2013)	0.4282	0.4275	0.4260	0.4238	0.4192	0.4081

Table 9 Continued

b/a	Theory	P					
		0.1	0.3	0.5	0.7	1.0	1.5
2	Present Model	0.3807	0.3800	0.3787	0.3768	0.3727	0.3628
	Quasi-3D (Mantari 2012)	0.3817	0.3811	0.3798	0.3778	0.3737	0.3638
	HSDT (Hassaine Daouadji 2013)	0.3806	0.3800	0.3786	0.3767	0.3726	0.3627
1	Present Model	0.2379	0.2375	0.2366	0.2354	0.2328	0.2267
	Quasi-3D (Mantari 2012)	0.2385	0.2381	0.2373	0.2361	0.2335	0.2273
	HSDT (Hassaine Daouadji 2013)	0.2378	0.2374	0.2366	0.2354	0.2328	0.2266

Table 10 Dimensionless fundamental frequency $\overline{\omega}$ of square plates

Theory	P=0		P=1			a/h=5		
	$a/h=\sqrt{10}$	a/h=10	a/h=5	a/h=10	a/h=20	P=2	P=2	P=2
Present Model	0.4660	0.0578	0.2192	0.0597	0.0153	0.2201	0.2214	0.2225
3D (Zenkour 2007)	0.4658	0.0578	0.2192	0.0596	0.0153	0.2197	0.2211	0.2225
HSDT (Hassaine Daouadji 2013)	0.4622	0.0577	0.2169	0.0592	0.0152	0.2178	0.2193	0.2206
Quasi-3D (Mantari 2012)	-	-	0.2193	0.0596	0.0153	0.2198	0.2212	0.2225
Quasi-3D (Neves 2012)	-	-	0.2193	0.0596	0.0153	0.2201	0.2216	0.2230
Quasi-3D (Neves 2013)	-	-	0.2193	-	-	0.2200	0.2215	0.2230

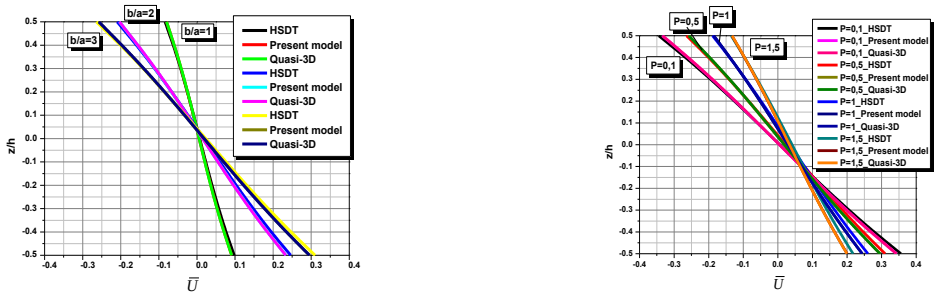

(a) Square plates a/h=4, P=0.5 (b) E-FGM rectangular plates; a/h=4, b=3a

Fig. 4 Variation of non-dimensional displacement $\overline{U}$ through the thickness

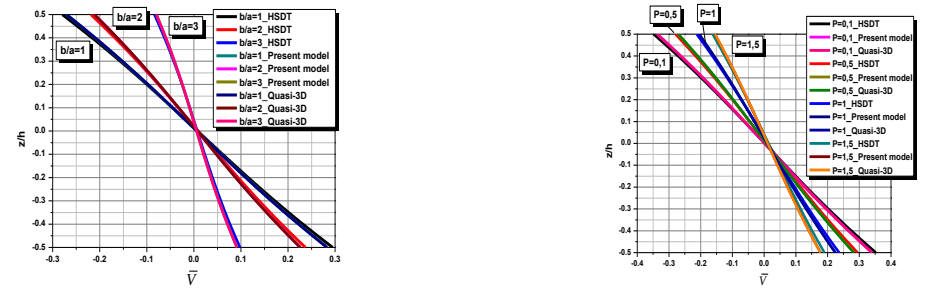

(a) Square plates a/h=4, P=0.5 (b) E-FGM rectangular plates; a/h=4, b=3a

Fig. 5 Variation of non-dimensional displacement $\overline{V}$ through the thickness

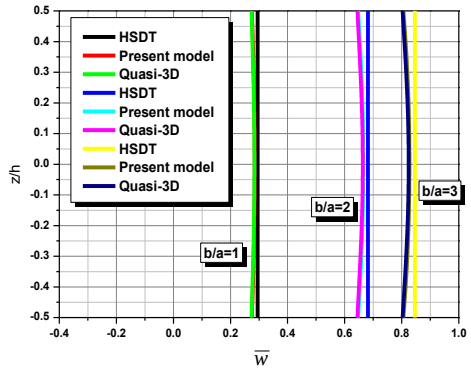

(a) Square plates a/h=4, P=0.5

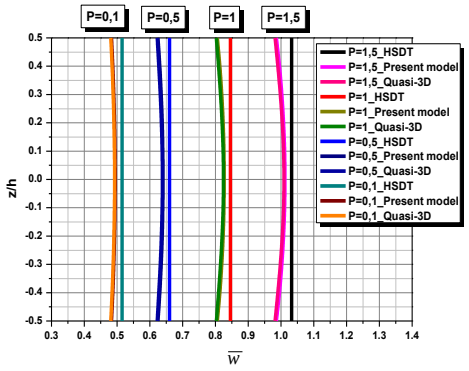

(b) E-FGM rectangular plates; a/h=4, b=3a

Fig. 6 Variation of non-dimensional deflection $\overline{w}$ through the thickness

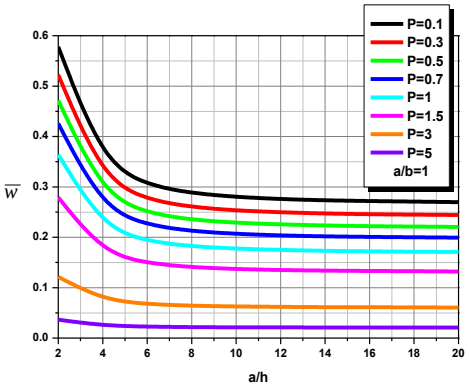

(a) variation $\overline{w}$ as a function of the side-to-thickness ratio a/h of FGM square plate ($\varepsilon_z \neq 0$)

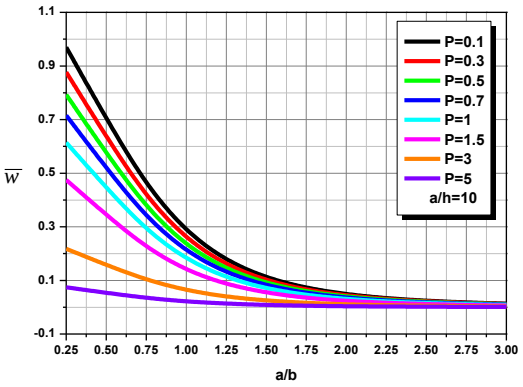

(b) variation $\overline{w}$ as a function of aspect ratio a/b of FGM rectangular plate ($\varepsilon_z \neq 0$)

Fig. 7 Dimensionless center deflection $\overline{w}$ plate using the present model ($\varepsilon_z \neq 0$)

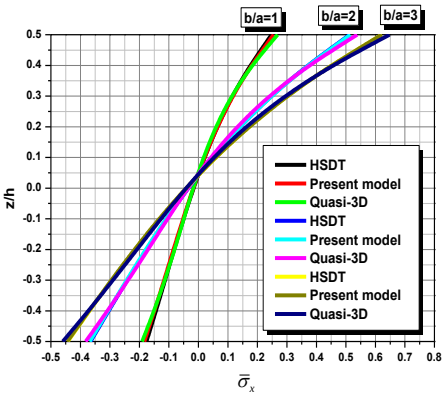

(a) Square plates a/h=4, P=0.5

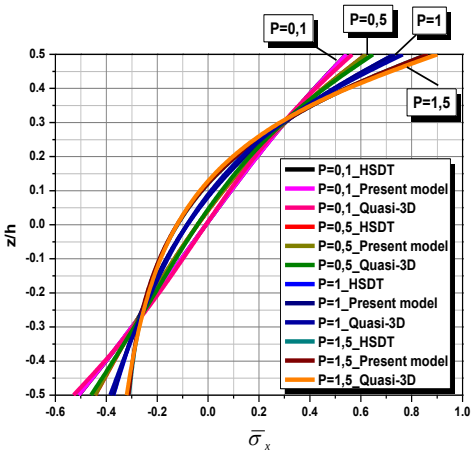

(b) E-FGM rectangular plates; a/h=4, b=3a

Fig. 8 Variation of axial stress $\overline{\sigma}_x$ through the thickness

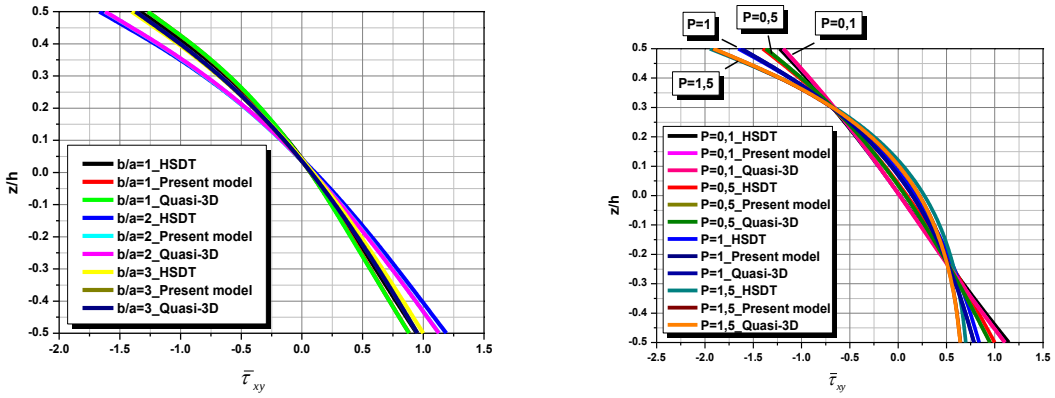

(a) Square plates a/h=4, P=0.5 (b) E-FGM rectangular plates; a/h=4, b=3a

Fig. 9 Variation of longitudinal shear stress $\bar{\tau}_{xy}$ through the thickness

3.2 Numerical results for vibration analysis

The accuracy of the present model proposed quasi-3D trigonometric higher order shear and normal deformation theory is also verified with free vibration analysis of a simply supported FGM plate. The effective Young's modulus is estimated using the power law distribution with Mori-Tanaka scheme (1973) in Eq. (17). Table 10 contains the dimensionless fundamental frequencies of square Al/ZrO_2 plate.

This approach has also been used by many other investigators and is applicable in zones of graded microstructure which possess a well-defined continuous matrix and a discontinuous particulate phase. It models with sufficient robustness the interaction of the elastic fields among neighboring inclusions. The non-dimensional fundamental frequency $\bar{\omega}$ is given in Table 10 for different values of thickness ratio and power law index. It is evident that the present model is in an excellent agreement with the 3D solutions (Mantari 2012) and quasi-3D solutions (Neves 2012).

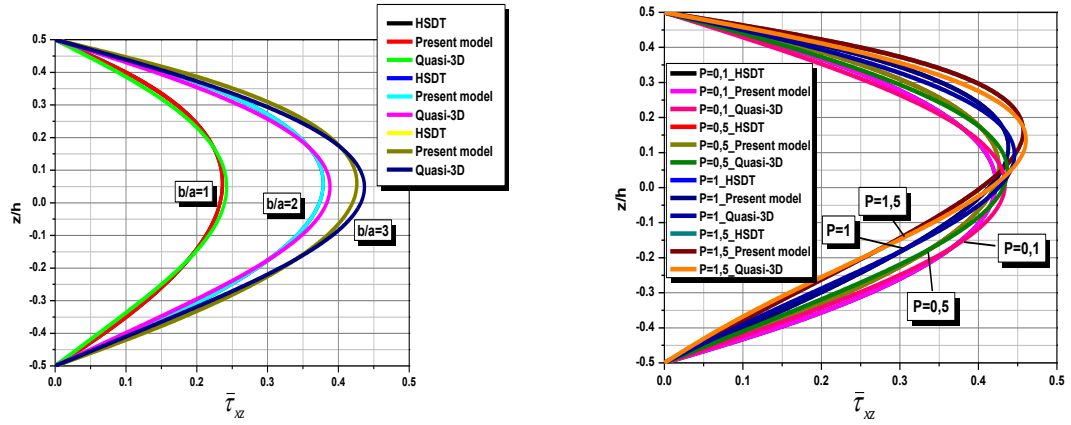

(a) Square plates a/h=4, P=0.5 (b) E-FGM rectangular plates; a/h=4, b=3a

Fig. 10 Variation of transversal shear stress $\bar{\tau}_{xz}$ through the thickness

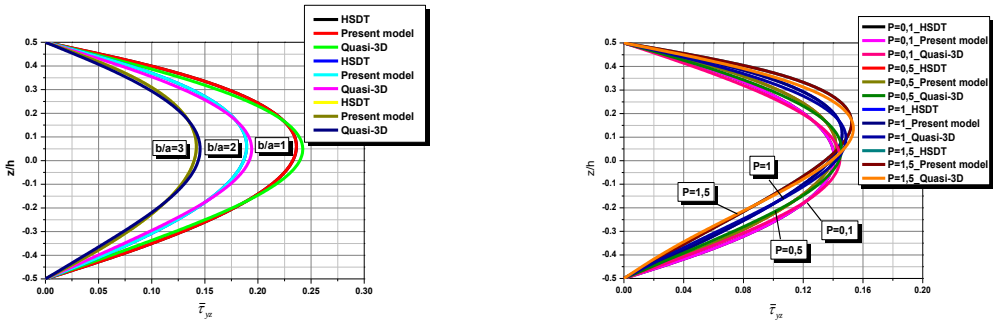

(a) Square plates a/h=4, P=0.5 (b) E-FGM rectangular plates; a/h=4, b=3a

Fig. 11 Variation of transversal shear stress $\bar{\tau}_{yz}$ through the thickness

4. Conclusions

We have considered a quasi-3D trigonometric higher order shear and normal deformation theory for the thickness stretching effect has been derived for bending and vibration analyses for simply supported functionally graded rectangular plates. The effective material properties at points in the plate are assumed to vary in the thickness direction only according to a simple exponential law. The theory accounts for the stretching and shear deformation effects without requiring a shear correction factor. By dividing the transverse displacement into bending, shear and stretching components, the number of unknowns and governing equations of the present theory is reduced to five and is therefore less than alternate theories available in the scientific literature. From the present analytical, it is evident that the thickness stretching effect is more pronounced for thick plates and it needs to be taken into consideration in more physically realistic simulations. The results predicted by the proposed theory are in an excellent agreement with 3D solutions and the thickness stretching effect is more pronounced for thick plates and it needs to be taken in consideration in the modeling. Numerical results show that the proposed quasi-3D trigonometric higher order shear and normal deformation theory is not only accurate but also provides an elegant and easily implementable approach for simulating bending and vibration behaviors of FGM plates.

Acknowledgments

The authors thank the referees for their valuable comments.

References

Abdelhak, Z., Hadji, L., Hassaine Daouadji, T. and Adda bedia, E.A. (2016), "Analysis of buckling response of functionally graded sandwich plates using a refined shear deformation theory", *Wind. Struct.*, **22**(3), 291-305.

Abrate, S. (2008), "Functionally graded plates behave like homogeneous plates", *Compos. Part B*, **39**(1),151-158.

Adim, B., Hassaine Daouadji, T. and Rabahi, A. (2016), "A simple higher order shear deformation theory for mechanical behavior of laminated composite plates", *Int. J. Adv. Struct. Eng.*, IJAS, **8**(2), 103-117.

Ait Atmane, H., Tounsi, A., Mechab, I. and Adda Bedia, E.A. (2010), "Free vibration analysis of functionally graded plates resting on Winkler-Pasternak elastic foundations using a new shear deformation theory", *Int. J. Mech. Mat*., **6**(2), 113-121.

Ait Yahia, S., Ait Atmane, H., Houari, M.S.A. and Tounsi, A. (2015), "Wave propagation in functionally graded plates with porosities using various higher-order shear deformation plate theories", *Struct. Eng. Mech.*, **53**(6), 1143-1165.

Baghdadi, H., Tounsi, A., Zidour, M. and Benzair, A. (2015), "Thermal effect on vibration characteristics of armchair and zigzag single-walled carbon nanotubes using nonlocal parabolic beam theory", *Fullerenes, Nanotube. Carbon Nanostruct.*, **23**(3), 266-272.

Benferhat, R., Hassaine Daouadji, T. and Said Mansour, M. (2016), "Effect of porosity on the bending and free vibration response of functionally graded plates resting on Winkler-Pasternak foundations", *Earthq. Struct.*, **10**(5), 1429-1449.

Bensattalah, T., Zidour, M., Tounsi, A. and Bedia, E.A.A. (2016), "Investigation of thermal and chirality effects on vibration of single-walled carbon anotubes embedded in a polymeric matrix using nonlocal elasticity theories", *Mech. Compos. Mater.*, **52**(4), 1-14.

Bhimaraddi, A. and Stevens, L. (1984), "A higher order theory for free vibration of orthotropic, homogeneous, and laminated rectangular plates", *J. Appl. Mech*., ASME, **51**(1), 195-198.

Bellifa, H., Benrahou, K.H.L., Hadji, Houari, M.S.A. and Tounsi, A. (2015), "Bending and free vibration analysis of functionally graded plates using a simple shear deformation theory and the concept the neutral surface position", *J. Brazil. Soc. Mech. Sci. Eng.*, **38**(1), 265-275.

Bennoun, M., Houari, M.S.A. and Tounsi, A. (2016), "A novel five variable refined plate theory for vibration analysis of functionally graded sandwich plates", *Mech. Adv. Mater. Struct.*, **23**(4), 423-431.

Boumia, L., Zidour, M., Benzair, A. and Tounsi, A. (2014), "A Timoshenko beam model for vibration analysis of chiral single-walled carbon nanotubes", *Physica E: Low-dimensional Syst. Nanostruct.*, **59**, 186-191.

Bouazza, M., Amara, K., Zidour, M., Tounsi, A. and Adda Bedia, El A. (2015), "Postbuckling analysis of functionally graded beams using hyperbolic shear deformation theory", *Rev. Inform. Eng. Appl.*, **2**(1), 1-14.

Bouazza, M., Amara, K., Zidour, M., Tounsi, A. and Adda Bedia, El A. (2015), "Postbuckling analysis of nanobeams using trigonometric Shear deformation theory", *Appl. Sci. Report.*, **10**(2), 112-121.

Bouazza, M., Amara, K., Zidour, M., Tounsi, A. and Adda Bedia, El A. (2014), "Hygrothermal effects on the postbuckling response of composite beams", *Am. J. Mater. Res.*, **1**(2), 35-43.

Carrera, E., Brischetto, S., Cinefra, M. and Soave, M. (2011), "Effects of thickness stretching in functionally graded plates and shells", *Comp. Part B: Eng*., **42**(2), 23-133.

Carrera, E. and Ciuffreda, A. (2005), "A unified formulation to assess theories of multilayered plates for various bending problems", *Compos. Struct*., **69**(3), 271-293.

Carrera, E., Brischetto, S. and Nali, P. (2011), *Plates and shells for smart structures: classical and advanced theories for modeling and analysis*, New York, USA, John Wiley & Sons.

Gafour, F., Zidour, M., Tounsi, A., Heireche, H. and Semmah, A. (2015), "Sound wave propagation in zigzag double-walled carbon nanotubes embedded in an elastic medium using nonlocal elasticity theory", *Physica E: Low-dimensional Syst. Nanostruct.*, **48**, 118-123.

Feldman, E. and Aboudi, J. (1997), "Buckling analysis of functionally graded plates subjected to uniaxial loading", *Compos. Struct*., **38**(1-4), 29-36.

Hamidi, A., Houari, M.S.A., Mahmoud, S.R. and Tounsi, A. (2015), "A sinusoidal plate theory with 5-unknowns and stretching effect for thermomechanical bending of functionally graded sandwich plates", *Steel Compos. Struct.*, **18**(1), 235-253.

Hassaine Daouadji, T. and Hadji, L. (2015), "Analytical solution of nonlinear cylindrical bending for functionally graded plates", *Geomech. Eng*., **9**(5), 631-644.

Hassaine Daouadji, T. and Adda bedia, E.A. (2013), "Analytical solution for bending analysis of functionally graded plates", *Scientia Iranica, Trans. B: Mech. Eng.*, **20**(3), 516-523.

Lo, K.H., Christensen, R.M. and Wu, E.M. (1977), "A high-order theory of plate deformation-part 2:

laminated plates", *J. Appl. Mech*., ASME, **44**(4), 669-674.
Mahi, A., Adda Bedia, E. and Tounsi, A. (2015), "A new hyperbolic shear deformation theory for bending and free vibration analysis of isotropic, functionally graded, sandwich and laminated composite plate", *Appl. Math. Model.*, **39**(9), 2489-2508.
Matsunaga, H. (2009), "Stress analysis of functionally graded plates subjected to thermal and mechanical loadings", *Compos. Struct*., **87**(4), 344-357.
Menaa, R., Tounsi, A., Mouaici, F., Mechab, I., Zidi, M. and Adda Bedia, E.A. (2012), "Analytical solutions for static shear correction factor of functionally graded rectangular beams", *Mech. Adv. Mater. Struct*., **19**(8), 641-652.
Mindlin, R.D. (1951), "Influence of rotary inertia and shear on flexural motions of isotropic elastic plates", *J. Appl. Mech*., ASME, **18**, 31-38.
Moradi, S. and Mansouri, M.H. (2012), "Thermal buckling analysis of shear deformable laminated orthotropic plates by differential quadrature", *Steel Compos Struct*., **12**, 129-147.
Mori, T. and Tanaka, K. (1973), "Average stress in matrix and average elastic energy of materials with misfitting inclusions", *Acta Metall*, **21**(5), 571-574.
Neves, A.M.A., Ferreira, A.J.M., Carrera, E., Cinefra, M., Roque, C.M.C. and Jorge, R.M.N. (2013), "Free vibration and buckling analysis of isotropic and sandwich functionally graded plates using a quasi-3D higher-order shear deformation theory and a meshless technique", *Compos. Part B: Eng*., **44**(1), 657-674.
Nelson, R.B., Lorch, D.R. (1974), "A refined theory for laminated orthotropic plates", *J. Appl. Mech*., ASME, **41**(1), 177-184.
Qian, L.F., Batra, R.C. and Chen, L.M. (2004), "Static and dynamic deformations of thick functionally graded elastic plates by using higher-order shear and normal deformable plate theory and meshless local Petrov-Galerkin method", *Compos. Part B: Eng*., **35**(6), 685-697.
Rashidi, M.M., Shooshtari, A. and Anwar, Bég O. (2012), "Homotopy perturbation study of nonlinear vibration of Von Kármán rectangular plates", *Comput. Struct*., **106-107**, 46-55.
Reissner, E. (1945), "Reflection on the theory of elastic plates", *J. Appl. Mech*., ASME, **38**(11), 1453-1464.
Reddy, J.N. (1984), "A simple higher-order theory for laminated composite plates", *J. Appl. Mech*., ASME, **51**(4), 745-752.
Reddy, J.N. (2000), "Analysis of functionally graded plates", *Int. J. Num. Meth. Eng*., **47**(1-3), 663-684.
Reddy, J.N. (2011), "A general nonlinear third-order theory of functionally graded plates", *Int. J. Aerosp. Lightweight Struct*., **1**(1), 1-21.
Mantari, J.L. and Guedes Soares, C. (2012), "Generalized hybrid quasi-3D shear deformation theory for the static analysis of advanced composite plates", *Compos. Struct*., **94**(8), 2561-2575.
Thai, H.T. and Kim, S.E. (2013), "A simple quasi-3D sinusoidal shear deformation theory for functionally graded plates", *Compos. Struct*., **99**, 172-180.
Tlidji, Y., Hassaine Daouadji, T., Hadji, L. and Adda bedia E.A. (2014), "Elasticity solution for bending response of functionally graded sandwich plates under thermo mechanical loading", *J. Therm. Stress*, **37**(7), 852-869.
Yaghoobi, H. and Yaghoobi, P. (2013), "Buckling analysis of sandwich plates with FGM face sheets resting on elastic foundation with various boundary conditions: an analytical approach", *Meccanica*, **48**(8), 2019-2035.
Zenkour, A. (2007), "Trigonometric Benchmark. Benchmark trigonometric and 3-D elasticity solutions for an exponentially graded thick rectangular plate", *Arch. Appl. Mech*., **77**(4), 197-214.
Zenkour, A.M. (2006), "Generalized shear deformation theory for bending analysis of functionally graded plates", *Appl. Math. Model.*, **30**(1), 67-84.
Zidour, M., Benrahou, K.H., Tounsi, A., Bedia, E.A.A. and Hadji, L. (2014), "Buckling analysis of chiral single-walled carbon nanotubes by using the nonlocal Timoshenko beam theory", *Mech. Compos. Mater*., **50**(1), 95-104.